

Available online at [www.sciencerepository.org](http://www.sciencerepository.org)

Science Repository



## Research Article

# Water-soluble SCR7 Can Abrogate DNA End Joining and Induce Cancer Cell Death

Ujjayinee Ray<sup>1</sup>, Anjana Elizabeth Jose<sup>1</sup>, Rohini Suresh<sup>1</sup>, Uthara Kaloor<sup>1</sup>, Hassan A. Swarup<sup>1</sup>, Mridula Nambiar<sup>1,2</sup> and Sathees C. Raghavan<sup>1\*</sup>

<sup>1</sup>Department of Biochemistry, Indian Institute of Science, Bangalore, India

<sup>2</sup>Department of Biology, Indian Institute of Science, Education and Research, Pune, India

## ARTICLE INFO

## Article history:

Received: 9 June, 2020

Accepted: 1 July, 2020

Published: 16 July, 2020

## Keywords:

NHEJ inhibitor

DSB repair

nonhomologous end joining

ligase IV

apoptosis

cancer therapy

## ABSTRACT

Small molecule inhibitors targeting DNA repair pathways in cancer cells is a novel and promising approach in cancer therapy, which can improve current therapeutic regimen. Although various attempts have been made for designing inhibitors against DNA damage response and repair proteins, reports on Nonhomologous End Joining (NHEJ) inhibitors are limited. Of the several chemical moieties identified, SCR7 and its oxidized form are novel and potent DNA Ligase IV inhibitors involved in the abrogation of DNA end joining thereby leading to cell death. In the present study, we have synthesized sodium salt of SCR7 to generate a water-soluble version of the molecule, referred to as water-soluble SCR7 (WS-SCR7). WS-SCR7 inhibits NHEJ in Ligase IV dependent manner, with a subtle effect on Ligase III at higher concentration. No effect on Ligase I mediated joining was observed. WS-SCR7 shows cytotoxicity in cancer cell lines, leading to induction of apoptosis in a dose-dependent manner.

© 2020 Sathees C. Raghavan. Hosting by Science Repository.

## Introduction

DNA double-strand breaks (DSBs) are the most deleterious DNA damage. When left unrepaired, DSBs can result in the accumulation of DNA breaks in the nucleus, chromosomal rearrangements and cell death [1, 2]. It is well established that induction of DSBs in cancer cells during radiotherapy or chemotherapy can lead to apoptosis and cell death. Recently, inhibition of DNA repair resulting in accumulation of DSBs is considered as an interesting and novel strategy to treat cancer [3, 4].

Repair of double-strand breaks occurs through two predominant pathways: Homologous Recombination (HR) and Nonhomologous DNA End joining (NHEJ) [5-9]. While HR requires homologous sequences from sister chromatid for the repair of DSBs, NHEJ is error-prone, sequence-independent and considered as a dynamic process involving the organization of multiple proteins [4, 10-13]. In the case of canonical NHEJ, one of the core proteins KU heterodimer binds to

broken DNA, followed by processing of the ends by DNA-PKcs, Artemis, and finally ligation by Ligase IV/XRCC4/XLF [4, 10-13]. The majority of DSBs generated in human cells are repaired through NHEJ.

Over the years therapeutic success of inhibition of DNA repair pathways depends on the selection of an appropriate protein target that is either directly involved in oncogenesis or has synthetic lethal interactions with another repair protein [4]. Previous reports have revealed a novel small molecule inhibitor, SCR7, which can inhibit NHEJ in a Ligase IV dependent manner in human cells [14]. Studies in mouse tumor models have suggested its therapeutic potential by regression of tumor volume and increasing the lifespan. Recently, we have shown that parental SCR7 can get cyclized into a stable form with the same molecular formula and mass, which upon further oxidation can result in SCR7-pyrazine, which possesses a different molecular formula and molecular weight [15]. Although both forms of SCR7 inhibited NHEJ *in vitro* and *ex vivo*, SCR7-pyrazine was less specific inside the cells [15].

\*Correspondence to: Sathees C. Raghavan, Department of Biochemistry, Indian Institute of Science, Bangalore-560012, India; Tel: 9180 22932674; E-mail: [sathees@iisc.ac.in](mailto:sathees@iisc.ac.in)

Multiple studies have also used SCR7 as a cancer therapeutic agent as well as a biochemical inhibitor [16-20]. Besides, several independent groups have reported a 2-19 fold increase in precise genome editing when SCR7 was used along with CRISPR-Cas9 constructs *ex vivo* and *in vivo* [3, 21-23].

Although SCR7 found multiple applications, its high hydrophobicity and DMSO solubility are few of the limitations for its clinical trial. In the present study, a water-soluble version of SCR7 has been synthesized, generating sodium salt of SCR7 and characterized with respect to inhibition of end joining and effect on cancer cell proliferation. WS-SCR7 works in Ligase IV dependent manner, leading to accumulation of DSBs and improved cell death.

## Materials and Methods

### I Chemicals and Reagents

Analytical grade reagents and chemicals were procured from Sigma Chemical Co. (St. Louis, MO, USA) and Sisco Research Laboratories (Andheri East, Mumbai, India). DNA modifying enzymes were from NEB (Ipswich, Massachusetts, USA). Foetal Bovine Serum (FBS), antibiotics Penicillin and Streptomycin (PenStrep) and tissue culture media were purchased from Lonza (Walkersville, MD, USA). Radiolabeled nucleotide,  $\gamma^{32}\text{P}$ -ATP was purchased from BRIT (Hyderabad, India).

### II Cell Lines and Culture Conditions

Nalm6 (B cell precursor leukemia), CEM (T cell leukemia) and Molt4 cells were cultured in RPMI 1640 supplemented with 10% FBS and 100  $\mu\text{g}/\text{mL}$  of Penicillin G and Streptomycin. Human cervical cancer cell line, HeLa was cultured in DMEM containing 10% FBS and PenStrep. Cells were grown at 37°C in a humidified atmosphere containing 5%  $\text{CO}_2$ . HeLa, CEM, Molt4 were obtained from National Centre for Cell Science, Pune, India, while Nalm6 was from M. Lieber, USA.

### III Chemical Synthesis and General Procedures

All reactions were monitored using TLC, performed with E. Merck silica gel 60 F254 aluminium plates (Kenilworth, NJ, USA) and were visualized under UV light. The following mobile phases were employed for TLC: chloroform, methanol, hexane and ethyl acetate in different ratios.  $^1\text{H}$  NMR (400 MHz) spectra was recorded in DMSO- $d_6$  solutions on a 400 MHz and 100 MHz spectrometer. Chemical shifts are reported in  $\delta$  (ppm) relative to TMS as internal standard; coupling constants (J) are expressed in Hz.

### IV Synthesis of SCR6 [3]

A suspension of 5,6-diamino-4-hydroxy-2-mercaptopyrimidine (1.0 g, 0.0063 mol) and benzaldehyde (0.67 g, 0.0063mol) in dimethyl formamide (30 mL) and acetic acid (10 mL) was stirred at room temperature for 16 h. The reaction mixture was then added slowly to ice-cold water, and the precipitated solid was filtered, washed with water and recrystallized from dimethyl formamide-ethanol as described. Yield: 0.93g (60%).

### V Synthesis of SCR7 [4]

A suspension of SCR6 [3] (0.93 g, 0.0037mol) and benzaldehyde (0.4g,0.0037mol) in dimethyl formamide (30 mL) and acetic acid (3 mL) was refluxed at 200°C for 8 to 10 h. The reaction mixture was transferred to ice-cold water, and the precipitated solid was filtered, washed with water and recrystallized from dimethyl formamide-ethanol as described before [14, 15] Yield: 0.44 g (35%).

### VI Synthesis of Sodium Salt of 2-Mercapto-6,7-Diphenyl-7,8-Dihydropteridin-4-Ol [5]

A suspension of SCR7 [4] (0.44 g, 0.00131 mol) and NaOH (0.234 g, 0.00585 mol) in THF (30 mL) was refluxed at 50°C for 12 h. Evaporation of solvents resulted in a yellow solid, which was washed in ethanol. The solid precipitate was allowed to dry. Yield: 0.231 g (60%); Yellow solid;  $^1\text{H}$  NMR (400 MHz, DMSO- $d_6$ ): 9.82 (s, 1H), 8.13 (s, 1H), 7.84 (d, J = 4 Hz, 2H), 7.36–7.21 (m, 8H). 5.92 (s,1H).

### VII Ethics Statement

Wistar rats were maintained according to the guidelines of the Animal Ethical Committee, Indian Institute of Science. Indian National Law on animal care and usage was followed. The study design was approved by the Institutional Animal Ethics Committee (CAF/Ethics/526/2016), Indian Institute of Science, Bangalore, India.

### VIII DNA End Joining Reactions Using Oligomeric DNA Substrate and Cell-Free Extracts

4-6 week old male Wistar rats, *Rattus norvegicus* were maintained in the Central Animal Facility, Indian Institute of Science, and organs were isolated following dissection. Rat testicular extract was prepared as described earlier [24-26].

Oligomeric DNA was purified using 8-12% denaturing PAGE as described earlier [27]. The 5' end-labeling of the oligomeric DNA was performed using T4 polynucleotide kinase in a buffer containing 20 mM Tris-acetate (pH 7.9), 10 mM magnesium acetate, 50 mM potassium acetate, 1 mM DTT and  $\gamma^{32}\text{P}$ -ATP at 37°C for 1 h. Next,  $\gamma^{32}\text{P}$ -ATP end-labeled 75 nt oligomer was annealed with the unlabeled complementary oligomer in 10 mM NaCl and 1 mM EDTA in a boiling water bath for 10 min, followed by slow cooling [28].

DNA end joining reactions were performed in NHEJ buffer containing 30 mM HEPES-KOH (pH 7.9), 7.5 mM  $\text{MgCl}_2$ , 1 mM DTT, 2 mM ATP, 50  $\mu\text{M}$  dNTPs and 0.1  $\mu\text{g}$  BSA at 25°C. The reaction mix containing tissue extract (1  $\mu\text{g}$ ) was incubated for 30 min with the inhibitor, followed by the addition of radiolabeled substrate and further incubation for 1 h [14, 24, 26, 29]. Phenol/chloroform extraction was used to purify the reaction products, which were then resolved on 8% denaturing PAGE. The gel was dried, exposed, and the signal was detected using PhosphorImager FLA9000 (Fuji, Japan). Quantification of joined products was done using MultiGauge software and presented as PhotoStimulated Luminescence Unit (PSLU). GraphPad Prism (V5) software was used for calculating statistical significance.

## IX End Joining Mediated by DNA Ligases

DNA ligases were overexpressed and purified from bacteria [14, 30]. His-tagged Ligase IV/XRCC4 bicistronic vector (pMJ4052) was a kind gift from Dr. Mauro Modesti. DNA Ligases were purified using Ni-NTA and UnoSphere Q Anion exchange columns. End joining reactions were set up in NHEJ buffer with purified protein and inhibitor at 25°C for 30 min, followed by incubation with radiolabeled nicked DNA substrate for 1 h. Reaction products were resolved on 12% denaturing PAGE, the signal was detected using PhosphorImager FLA9000 (Fuji, Japan) and analysed using GraphPad Prism (V5) software.

## X Cytotoxicity

Cell viability was analysed by Trypan Blue dye exclusion assay as described previously [14, 31-33]. Briefly, 25,000 cells/ml were seeded in tissue culture grade 24-well plate and incubated for 48 h with varying concentrations of WS-SCR7 (10, 50, 100 and 250  $\mu$ M). Cells were mixed with an equal volume of 0.4% Trypan blue (Sigma Chemical Co., St Louis, MO, USA) and counted using haemocytometer. Experiments were repeated three times, and error bars plotted using GraphPad Prism (V5) software.

## XI Cell Cycle Analysis

Cell cycle analysis was performed as described before [34, 35]. Briefly, 25,000 cells/ml were seeded in 4 ml culture media and treated with WS-SCR7 (90 and 180  $\mu$ M for Molt4) for 48 h. Harvested cells were washed with 1X PBS and fixed in 70% ethanol overnight at -20°C. Fixed samples were centrifuged and subjected to RNaseA treatment overnight under shaking conditions at 37°C. Finally, cells were stained with Propidium Iodide and analysed using CytoFLEX flow cytometer, Beckman Coulter (Brea, California, United States). A minimum of 10,000 cells were acquired, and data analysis was done using CytExpert software.

## XII JC-1 assay

In order to identify changes in mitochondrial membrane potential, cells were treated with increasing concentration of WS-SCR7 (50 and 100  $\mu$ M for Nalm6) for 48 h and subjected to JC-1 staining assay [31, 36, 37]. Cells were incubated in JC-1 dye (5,5',6,6'-tetrachloro-1,1',3,3'-tetraethylbenzimidazolcarbocyanamideiodide (Calbiochem, USA) (1  $\mu$ M) at 37°C for 20 min, with intermittent mixing. 2, 4-Dinitrophenol (4 mM) was used as the positive control. After 1X PBS wash, samples were acquired using CytoFLEX flow cytometer. Mitochondrial depolarization, indicated by a decrease in the red/green fluorescence intensity ratio, was represented in bar diagrams prepared using GraphPad Prism.

## Results and Discussion

In our previous studies, we have reported SCR7 and its other forms as novel and potent inhibitor of NHEJ that can work in Ligase IV dependent manner [14, 15, 38]. SCR7 binds to the DNA binding domain of Ligase IV, thereby interfering with the binding of the protein to DSBs, leading to accumulation of unrepaired breaks inside cells and apoptosis. However, a major limitation of the molecule was its solubility in organic

solvents such as DMSO. In order to increase its solubility and hence permeability in cells, a water-soluble version of SCR7 was synthesized by replacing one of the hydrogens with sodium in the moiety (Figure 1A). Molecular structure was verified using NMR studies (Figure 1B).

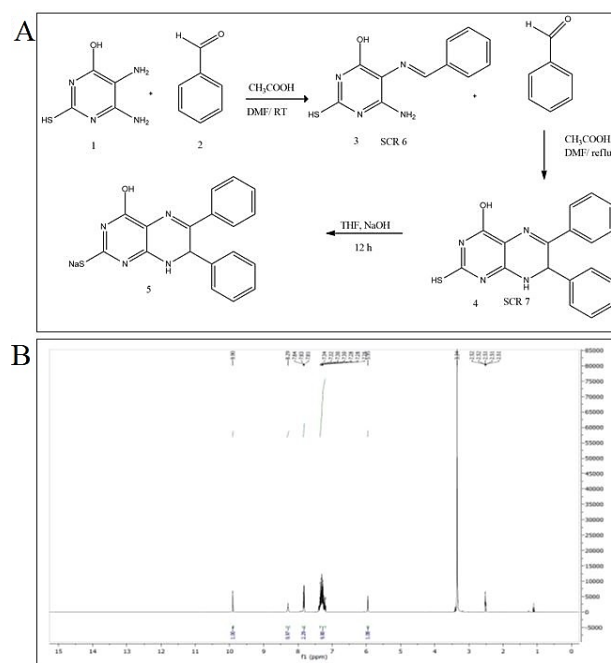


**Figure 1:** Synthesis and characterization of WS-SCR7. **A)** Synthetic route employed in obtaining WS-SCR7. **B)** Structural characterization of WS-SCR7 by  $^1\text{H}$ -NMR spectroscopy.

A cell-free repair assay system was utilised to investigate the potential of WS-SCR7 to inhibit NHEJ. Previously, we have reported that testicular extracts are proficient in NHEJ compared to other tissue extracts [25, 26]. Hence, testicular extracts were incubated with increasing doses of WS-SCR7 (50, 100, 200, 400, 600, 800 and 1000  $\mu$ M). Results revealed inhibition of end joining from 600  $\mu$ M of WS-SCR7 onwards when the compound was incubated with  $\gamma^{32}$ -labeled double-stranded oligomeric DNA substrate in the presence of testicular proteins (Figure 2A). Ligase IV/XRCC4 is the crucial protein involved in ligation of breaks as the last step in the NHEJ pathway [39-42]. As reported earlier, SCR7 can inhibit purified Ligase IV/XRCC4 mediated joining at 200  $\mu$ M [14, 15]. In the present study, the effect of WS-SCR7 on the inhibition of joining catalysed by purified Ligase IV/XRCC4 was investigated (Figure 2B). Results revealed a dose-dependent inhibition of joining catalysed by Ligase IV/XRCC4 from 200  $\mu$ M, suggesting Ligase IV dependent effect of the water-soluble version at a concentration similar to that of SCR7. Effect of WS-SCR7 (50, 100, 200, 400, 600, 800 and 1000  $\mu$ M) on Ligase I and Ligase III/XRCC1 mediated end joining was also investigated. We observed that WS-SCR7 did not inhibit Ligase I mediated end joining even at the highest concentration (1000  $\mu$ M), similar to SCR7 (Figure 2C). However, Ligase III/XRCC1 catalysed end joining was inhibited from a concentration of 600  $\mu$ M onwards (Figure 2D), which was consistent with our previous report [14].

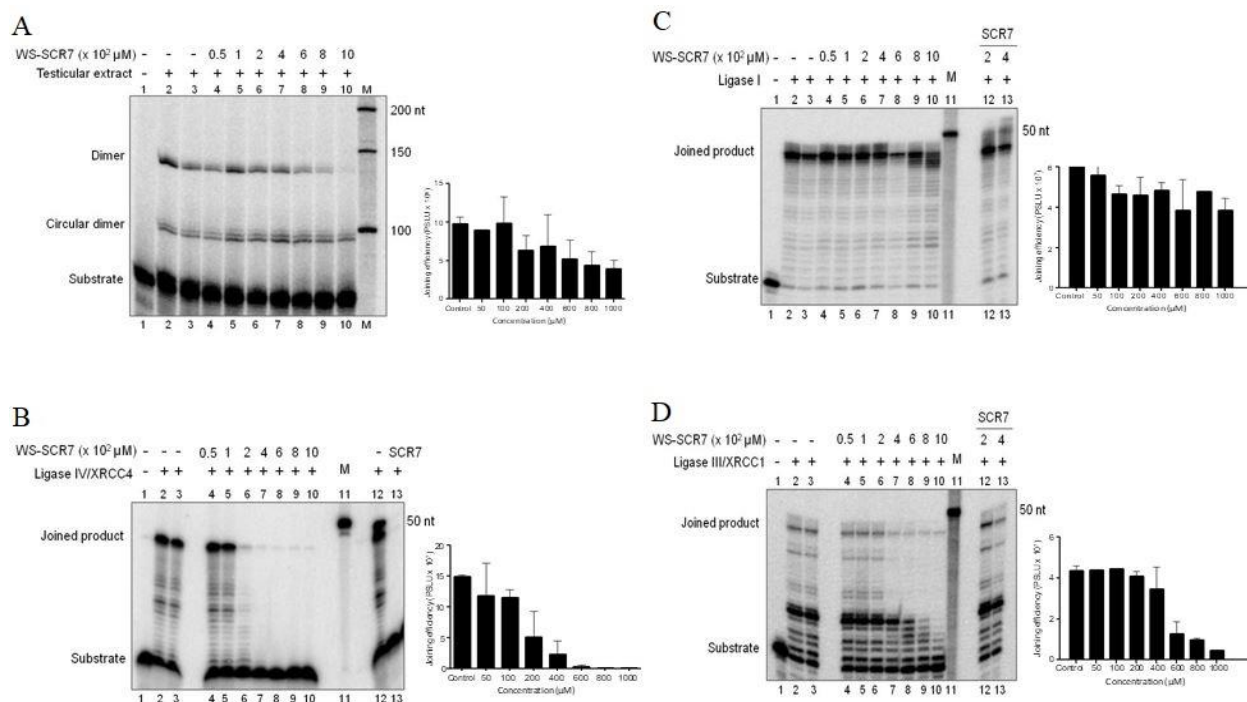


**Figure 2:** Effect of WS-SCR7 on NHEJ and evaluation of Ligase IV specificity. **A)** Inhibition of end joining of rat testicular extract in presence of increasing concentrations of WS-SCR7 (50, 100, 200, 400, 600, 800 and 1000  $\mu\text{M}$ ). Bar graph shows quantification of inhibition of end joining in presence of WS-SCR7 in a concentration-dependent manner. **B)** Inhibition of joining catalysed by purified Ligase IV/XRCC4 when increasing concentrations (50, 100, 200, 400, 600, 800 and 1000  $\mu\text{M}$ ) of WS-SCR7 was added. Bar graph depicts quantification of inhibition of Ligase IV/XRCC4 mediated joining. **C)** Evaluation of effect of WS-SCR7 on joining catalysed by Ligase I. **D)** Evaluation of joining by Ligase III/XRCC1, in presence of WS-SCR7 and bar graphs showing quantification of extent of inhibition.

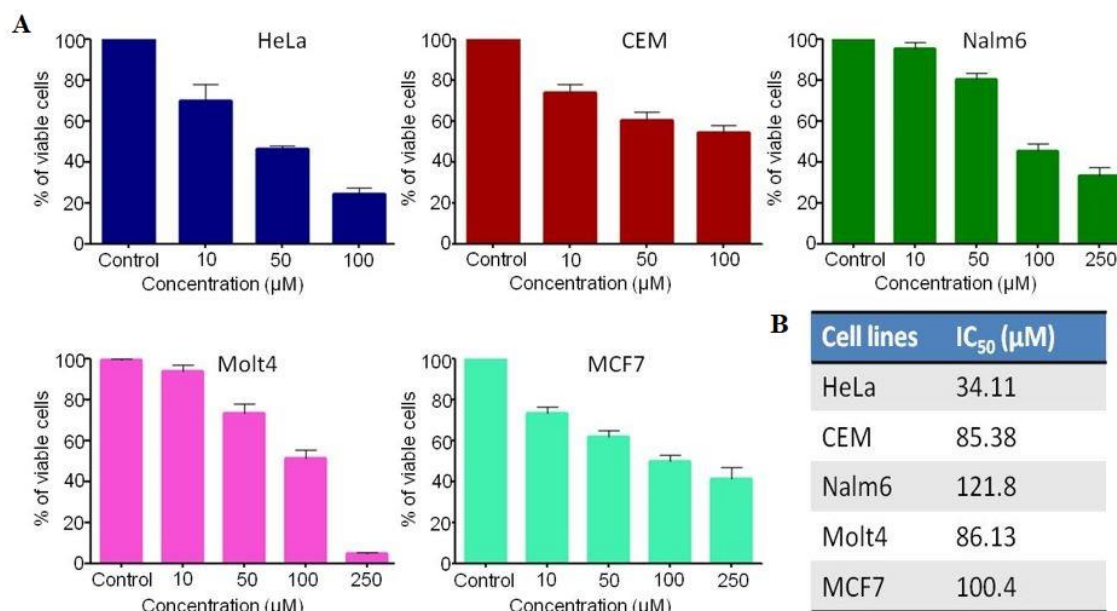


**Figure 3:** Evaluation of cytotoxicity induced by WS-SCR7 in cancer cell lines. **A)** Bar graphs representing cytotoxicity of WS-SCR7 (10, 50, 100 and 250  $\mu\text{M}$ ) after 48 h of treatment in various cancer cell lines, including HeLa, CEM, Nalm6, Molt4 and MCF7. **B)** Table representing IC<sub>50</sub> values (in  $\mu\text{M}$ ) of WS-SCR7 in various cancer cell lines at 48 h.

Cytotoxicity of WS-SCR7 was evaluated in various cancer cell lines (HeLa, CEM, Nalm6, Molt4 and MCF7) by incubating with increasing concentrations (10, 50, 100 and 250  $\mu\text{M}$ ), and IC<sub>50</sub> values were

determined (Figures 3A & 3B). Among the cell lines tested, cervical cancer cell line, HeLa showed the highest sensitivity, with an IC<sub>50</sub> of 34  $\mu\text{M}$  (Figures 3A & 3B), which was comparable to that of SCR7.



However, WS-SCR7 induced cytotoxicity was comparatively less in the case of other cell lines (Figures 3A & 3B).

In order to investigate the effect of WS-SCR7 on cell cycle progression in cancer cells, Molt4 was treated with increasing concentrations of the inhibitor (0, 90 and 180  $\mu$ M) (Figure 4A). Results revealed an increase in the SubG1 population upon treatment with WS-SCR7 in a dose-dependent manner. A subtle S-phase arrest was also observed (Figure 4A). The effect of WS-SCR7 on mitochondrial membrane potential was

evaluated by JC-1 assay in Nalm6 (Figure 4B) at different concentrations (0, 50 and 100  $\mu$ M). 2, 4-DNP, an uncoupler was used as positive control and showed more than 50% depolarisation of mitochondria. A shift from red to green population in WS-SCR7 treated samples suggested an increase in depolarised mitochondrial membrane potential in a dose-dependent manner (Figure 4B). Overall, WS-SCR7 can inhibit end joining in Ligase-IV dependent manner similar to SCR7 and induce cell death in cancer cells.

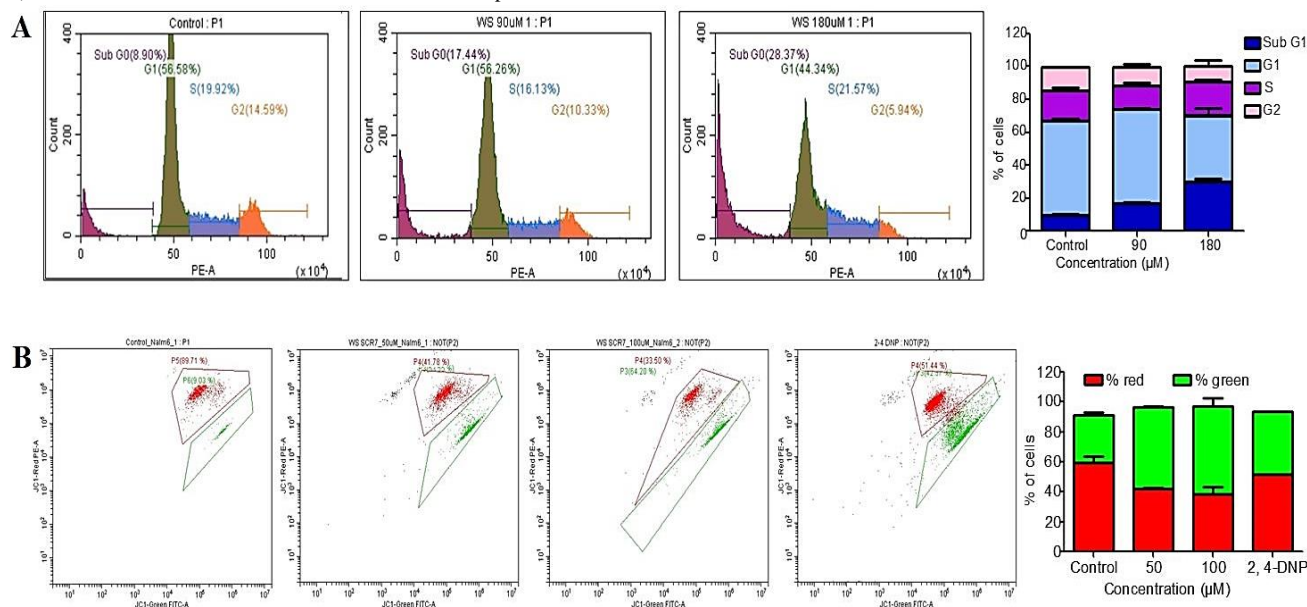


**Figure 4:** Evaluation of effect of WS-SCR7 in cancer cell lines. **A)** Analysis of cell cycle progression in Molt4 cells after treatment with WS-SCR7 in a dose-dependent manner (0, 90, 180  $\mu$ M). Percentage of cells in each stage of cell cycle following treatment with WS-SCR7 for 48 h is represented as bar graphs. **B)** JC-1 assay for detecting loss of mitochondrial membrane potential in Nalm6 cells post-treatment with WS-SCR7 in a dose-dependent manner (0, 50 and 100  $\mu$ M for 48 h). 2, 4-DNP (4 mM) serves as positive control. Bar graphs depict percentage of green cells undergoing loss in membrane potential to that of red cells.

DNA repair inhibitors are considered as attractive cancer therapeutic agents owing to the upregulation of several repair proteins in cancer. Being one of the major DSB repair pathways in mammals, the upregulation of NHEJ has been shown to provide resistance to various cancer cells [43]. Reports suggest upregulation of KU and DNA-PKcs in breast, gastric, lung and esophageal cancers, and polymorphisms in Ligase IV and XRCC4 [4, 44-46]. Current literature in the field offers very few reports on the characterization of inhibitors targeting Ligase IV, a crucial protein involved in resealing of breaks at the last step of the NHEJ pathway. In this line, SCR7 and its forms are considered potent NHEJ inhibitors that can work in a Ligase IV dependent manner [14, 15]. The abrogation of NHEJ led to increased cytotoxicity and tumor regression both inside the cell lines and *in vivo*. Further, a water-soluble version of SCR7-pyrazine (Na-SCR7-P) was synthesized and characterized. Na-SCR7-P inhibited end joining of all three Ligases and inhibited tumor progression in mice [38].

In the present study we have investigated the potential of water-soluble version of SCR7 in inhibition of end joining compared to its parental form that is DMSO soluble. Interestingly we found that WS-SCR7 can abrogate end joining mediated by Ligase IV/XRCC4 at a concentration similar to that of SCR7. Although no inhibition was observed with

respect to Ligase I mediated joining, WS-SCR7 inhibited Ligase III/XRCC1 at higher concentration, which was 3-fold higher than that for Ligase IV. We also observed that similar to DMSO soluble version, WS-SCR7 induced cytotoxicity in several cancer cell lines and could lead to the depolarisation of mitochondria suggesting activation of the intrinsic pathway of apoptosis. Consistently, an increase in the SubG1 population was also obtained, which along with observed ability of inhibition of NHEJ suggests the accumulation of DSBs leading to apoptosis.

## Acknowledgements

We thank Sumedha Dahal and other members of the SCR laboratory for comments on the manuscript. We thank Supriya Vartak for help in cell culture.

## Funding

The work was funded by grants from CEFIPRA (IFC/5203-4/2015/131), DAE (21/01/2016-BRNS/35074), DBT (BT/PR13458/COE/34/33/2015), IISc-DBT partnership programme

[DBT/BF/PR/INS/2011-12/IISc] to SCR. UR is supported by Senior Research fellowship (SRF) from CSIR, India.

### Conflicts of Interest

None.

### Author Contributions

SCR coordinated the study and provided the reagents; SCR, UR and MN designed the experiments, interpreted results and wrote the manuscript; UR and RP conducted the experiments; Chemical synthesis and characterization of the inhibitor were done by AEJ, UK and HAS.

### REFERENCES

1. J Wade Harper, Stephen J Elledge (2007) The DNA damage response: ten years after. *Mol Cell* 28: 739-745. [Crossref]
2. Mridula Nambiar, Sathees C Raghavan (2013) Chromosomal translocations among the healthy human population: implications in oncogenesis. *Cell Mol Life Sci* 70: 1381-1392. [Crossref]
3. Supriya V Vartak, Sathees C Raghavan (2015) Inhibition of nonhomologous end joining to increase the specificity of CRISPR/Cas9 genome editing. *FEBS J* 282: 4289-4294. [Crossref]
4. Mrinal Srivastava, Sathees C Raghavan (2015) DNA double-strand break repair inhibitors as cancer therapeutics. *Chem Biol* 22: 17-29. [Crossref]
5. Alberto Ciccica, Stephen J Elledge (2010) The DNA damage response: making it safe to play with knives. *Mol Cell* 40: 179-204. [Crossref]
6. Jiri Lukas, Claudia Lukas (2013) Molecular biology. Shielding broken DNA for a quick fix. *Science* 339: 652-653. [Crossref]
7. Pandey MR, S C (2017) DNA double-strand break repair in mammals. *J Radiat Cancer Res* 8: 93-97.
8. B Pardo, B Gómez González, A Aguilera (2009) DNA repair in mammalian cells: DNA double-strand break repair: how to fix a broken relationship. *Cell Mol Life Sci* 66: 1039-1056. [Crossref]
9. Sophie E Polo, Stephen P Jackson (2011) Dynamics of DNA damage response proteins at DNA breaks: a focus on protein modifications. *Genes Dev* 25: 409-433. [Crossref]
10. Peter Ahnesorg, Philippa Smith, Stephen P Jackson (2006) XLF interacts with the XRCC4-DNA ligase IV complex to promote DNA nonhomologous end-joining. *Cell* 124: 301-313. [Crossref]
11. Michael R Lieber (2010) The mechanism of double-strand DNA break repair by the nonhomologous DNA end-joining pathway. *Annu Rev Biochem* 79: 181-211. [Crossref]
12. Dylan A Reid, Michael P Conlin, Yandong Yin, Howard H Chang, Go Watanabe et al. (2017) Bridging of double-stranded breaks by the nonhomologous end-joining ligation complex is modulated by DNA end chemistry. *Nucleic Acids Res* 45: 1872-1878. [Crossref]
13. Chun J Tsai, Sunny A Kim, Gilbert Chu (2007) Cernunnos/XLF promotes the ligation of mismatched and noncohesive DNA ends. *Proc Natl Acad Sci U S A* 104: 7851-7856. [Crossref]
14. Mrinal Srivastava, Mridula Nambiar, Sheetal Sharma, Subhas S Karki, G Goldsmith et al. (2012) An inhibitor of nonhomologous end-joining abrogates double-strand break repair and impedes cancer progression. *Cell* 151: 1474-1487. [Crossref]
15. Supriya V Vartak, Hassan A Swarup, Vidya Gopalakrishnan, Vindya K Gopinatha, Virginie Ropars et al. (2018) Autocyclized and oxidized forms of SCR7 induce cancer cell death by inhibiting nonhomologous DNA end joining in a Ligase IV dependent manner. *FEBS J* 285: 3959-3976. [Crossref]
16. Vidya Gopalakrishnan, Gudapureddy Radha, Sathees C Raghavan, Bibha Choudhary (2018) Inhibitor of nonhomologous end joining can inhibit proliferation of diffuse large B-Cell lymphoma cells and potentiate the effect of ionization radiation. *J Radiat Cancer Res* 9: 93-101.
17. Ajay Kumar, Devyani Bhatkar, Devashree Jahagirdar, Nilesh Kumar Sharma (2017) Non-homologous End Joining Inhibitor SCR-7 to Exacerbate Low-dose Doxorubicin Cytotoxicity in HeLa Cells. *J Cancer Prev* 22: 47-54. [Crossref]
18. Dylan A Reid, Sarah Keegan, Alejandra Leo Macias, Go Watanabe, Natasha T Strande et al. (2015) Organization and dynamics of the nonhomologous end-joining machinery during DNA double-strand break repair. *Proc Natl Acad Sci U S A* 112: E2575-E2584. [Crossref]
19. Zhe Yang, Shihao Chen, Songlei Xue, Xinxu Li, Jiang Hu et al. (2018) Injection of an SV40 transcriptional terminator causes embryonic lethality: a possible zebrafish model for screening nonhomologous end-joining inhibitors. *Onco Targets Ther* 11: 4945-4953. [Crossref]
20. Vivek Tripathi, Himanshi Agarwal, Swati Priya, Harish Batra, Priyanka Modi (2018) MRN complex-dependent recruitment of ubiquitylated BLM helicase to DSBs negatively regulates DNA repair pathways. *Nat Commun* 9: 1016. [Crossref]
21. Van Trung Chu, Timm Weber, Benedikt Wefers, Wolfgang Wurst, Sandrine Sander et al. (2015) Increasing the efficiency of homology-directed repair for CRISPR-Cas9-induced precise gene editing in mammalian cells. *Nat Biotechnol* 33: 543-548. [Crossref]
22. Takeshi Maruyama, Stephanie K Dougan, Matthias C Truttmann, Angelina M Bilate, Jessica R Ingram et al. (2015) Increasing the efficiency of precise genome editing with CRISPR-Cas9 by inhibition of nonhomologous end joining. *Nat Biotechnol* 33: 538-542. [Crossref]
23. Priti Singh, John C Schimenti, Ewelina Bolcun Filas (2015) A mouse geneticist's practical guide to CRISPR applications. *Genetics* 199: 1-15. [Crossref]
24. Tadi Satish Kumar, Vijayalakshmi Kari, Bibha Choudhary, Mridula Nambiar, T S Akila et al. (2010) Anti-apoptotic protein BCL2 down-regulates DNA end joining in cancer cells. *J Biol Chem* 285: 32657-32670. [Crossref]
25. C R Sathees, M J Raman (1999) Mouse testicular extracts process DNA double-strand breaks efficiently by DNA end-to-end joining. *Mutat Res* 433: 1-13. [Crossref]
26. Sheetal Sharma, Bibha Choudhary, Sathees C Raghavan (2011) Efficiency of nonhomologous DNA end joining varies among somatic tissues, despite similarity in mechanism. *Cell Mol Life Sci* 68: 661-676. [Crossref]
27. Rupa Kumari, Sathees C Raghavan (2015) Structure-specific nuclease activity of RAGs is modulated by sequence, length and phase position of flanking double-stranded DNA. *FEBS J* 282: 4-18. [Crossref]
28. Mridula Nambiar, G Goldsmith, Balaji T Moorthy, Michael R Lieber, Mamata V Joshi (2011) Formation of a G-quadruplex at the BCL2 major breakpoint region of the t(14;18) translocation in follicular lymphoma. *Nucleic Acids Res* 39: 936-948. [Crossref]
29. Kishore K Chiruvella, Robin Sebastian, Sheetal Sharma, Anjali A Karande, Bibha Choudhary et al. (2012) Time-dependent

- predominance of nonhomologous DNA end-joining pathways during embryonic development in mice. *J Mol Biol* 417: 197-211. [[Crossref](#)]
30. Monica Pandey, Sujeet Kumar, Gunaseelan Goldsmith, Mrinal Srivastava, Santhini Elango et al. (2017) Identification and characterization of novel ligase I inhibitors. *Mol Carcinog* 56: 550-566. [[Crossref](#)]
  31. Kishore K Chiruvella, Vijayalakshmi Kari, Bibha Choudhary, Mridula Nambiar, Rama Gopal Ghanta et al. (2008) Methyl angolensate, a natural tetranortriterpenoid induces intrinsic apoptotic pathway in leukemic cells. *FEBS Lett* 582: 4066-4076. [[Crossref](#)]
  32. C V Kavitha, Mridula Nambiar, C S Ananda Kumar, Bibha Choudhary, K Muniyappa et al. (2009) Novel derivatives of spirohydantoin induce growth inhibition followed by apoptosis in leukemia cells. *Biochem Pharmacol* 77: 348-363. [[Crossref](#)]
  33. Mahesh Hegde, Kempegowda Mantelingu, Monica Pandey, Chottanahalli S Pavankumar, Kanchugarakoppal S Rangappa et al. (2016) Combinatorial Study of a Novel Poly (ADP-ribose) Polymerase Inhibitor and an HDAC Inhibitor, SAHA, in Leukemic Cell Lines. *Target Oncol* 11: 655-665. [[Crossref](#)]
  34. Shikha Srivastava, Ranganatha R Somasagara, Mahesh Hegde, Mayilaadumveetil Nishana, Satish Kumar Tadi et al. (2016) Quercetin, a Natural Flavonoid Interacts with DNA, Arrests Cell Cycle and Causes Tumor Regression by Activating Mitochondrial Pathway of Apoptosis. *Sci Rep* 6: 24049. [[Crossref](#)]
  35. Elizabeth Thomas, Vidya Gopalakrishnan, Ranganatha R Somasagara, Bibha Choudhary, Sathees C Raghavan (2016) Extract of Vernonia condensata, Inhibits Tumor Progression and Improves Survival of Tumor-allograft Bearing Mouse. *Sci Rep* 6: 23255. [[Crossref](#)]
  36. Supriya V Vartak, Mahesh Hegde, Divyaanka Iyer, Snehal Gaikwad, Vidya Gopalakrishnan et al. (2016) A novel inhibitor of BCL2, Disarib abrogates tumor growth while sparing platelets, by activating intrinsic pathway of apoptosis. *Biochem Pharmacol* 122: 10-22. [[Crossref](#)]
  37. C V Kavitha, Mridula Nambiar, Pavan B Narayanaswamy, Elizabeth Thomas, Ujjwal Rathore et al. (2013) Propyl-2-(8-(3,4-difluorobenzyl)-2',5'-dioxo-8-azaspiro[bicyclo[3.2.1] octane-3,4'-imidazolidine]-1'-yl) acetate induces apoptosis in human leukemia cells through mitochondrial pathway following cell cycle arrest. *PLoS One* 8: e69103. [[Crossref](#)]
  38. Monica Pandey, Vidya Gopalakrishnan, Hassan A Swarup, Sujeet Kumar, Radha Gudapureddy, Anjana Elizabeth Jose et al. (2019) Water-soluble version of SCR7-pyrazine inhibits DNA repair and abrogates tumor cell proliferation. *J Radiat Cancer Res* 10: 27-43.
  39. S E Crichtlow, R P Bowater, S P Jackson (1997) Mammalian DNA double-strand break repair protein XRCC4 interacts with DNA ligase IV. *Curr Biol* 7: 588-598. [[Crossref](#)]
  40. U Grawunder, D Zimmer, S Fugmann, K Schwarz, M R Lieber (1998) DNA ligase IV is essential for V(D)J recombination and DNA double-strand break repair in human precursor lymphocytes. *Mol Cell* 2: 477-484. [[Crossref](#)]
  41. S H Teo, S P Jackson (1997) Identification of *Saccharomyces cerevisiae* DNA ligase IV: involvement in DNA double-strand break repair. *EMBO J* 16: 4788-4795. [[Crossref](#)]
  42. T E Wilson, U Grawunder, M R Lieber (1997) Yeast DNA ligase IV mediates non-homologous DNA end joining. *Nature* 388: 495-498. [[Crossref](#)]
  43. Adrian C Begg, Fiona A Stewart, Conchita Vens (2011) Strategies to improve radiotherapy with targeted drugs. *Nat Rev Cancer* 11: 239-253. [[Crossref](#)]
  44. C Beskow, J Skikuniene, A Holgersson, B Nilsson, R Lewensohn et al. (2009) Radioresistant cervical cancer shows upregulation of the NHEJ proteins DNA-PKcs, Ku70 and Ku86. *Br J Cancer* 101: 816-821. [[Crossref](#)]
  45. S Pucci, P Mazzarelli, C Rabitti, M Giai, M Gallucci et al. (2001) Tumor specific modulation of KU70/80 DNA binding activity in breast and bladder human tumor biopsies. *Oncogene* 20: 739-747. [[Crossref](#)]
  46. Bettina Kuschel, Annika Auranen, Simon McBride, Karen L Novik, Antonis Antoniou et al. (2002) Variants in DNA double-strand break repair genes and breast cancer susceptibility. *Hum Mol Genet* 11: 1399-1407. [[Crossref](#)]